Hindawi Publishing Corporation
Journal of Nanomaterials
Volume 2013, Article ID 152079, 7 pages
http://dx.doi.org/10.1155/2013/152079

Research Article

pH-Sensing Characteristics of Hydrothermal Al-Doped ZnO Nanostructures

Jyh-Liang Wang,[1] Po-Yu Yang,[2] Tsang-Yen Hsieh,[1] Chuan-Chou Hwang,[1] and Miin-Horng Juang[3]

[1] *Department of Electronics Engineering, Ming Chi University of Technology, New Taipei 24301, Taiwan*
[2] *Department of Electronics Engineering and Institute of Electronics, National Chiao Tung University, Hsinchu 30010, Taiwan*
[3] *Department of Electronic Engineering, National Taiwan University of Science and Technology, Taipei 106, Taiwan*

Correspondence should be addressed to Jyh-Liang Wang; joewang@mail.mcut.edu.tw

Received 12 May 2013; Accepted 5 August 2013

Academic Editor: Tifeng Jiao

Highly sensitive and stable pH-sensing properties of an extended-gate field-effect transistor (EGFET) based on the aluminum-doped ZnO (AZO) nanostructures have been demonstrated. The AZO nanostructures with different Al concentrations were synthesized on AZO/glass substrate via a simple hydrothermal growth method at 85°C. The AZO sensing nanostructures were connected with the metal-oxide-semiconductor field-effect transistor (MOSFET). Afterwards, the current-voltage (*I-V*) characteristics and the sensing properties of the pH-EGFET sensors were obtained in different buffer solutions, respectively. As a result, the pH-sensing characteristics of AZO nanostructured pH-EGFET sensors with Al dosage of 3 at.% can exhibit the higher sensitivity of 57.95 mV/pH, the larger linearity of 0.9998, the smaller deviation of 0.023 in linearity, the lower drift rate of 1.27 mV/hour, and the lower threshold voltage of 1.32 V with a wider sensing range (pH 1 ~ pH 13). Hence, the outstanding stability and durability of AZO nanostructured ionic EGFET sensors are attractive for the electrochemical application of flexible and disposable biosensor.

1. Introduction

Ion-sensitive field-effect transistor (ISFET) was first fabricated as an alternative to the fragile glass electrode in pH-measurement and ion concentrations by Bergveld in 1970 [1]. The major difference between ISFET and usual metal-oxide-semiconductor field-effect transistor (MOSFET) is that there is no metal gate electrode in the former. The first pH-sensitive membrane to be used in ISFET was silicon dioxide (SiO_2), which showed an unstable sensitivity and large drift [1]. Silicon nitride (Si_3N_4) and aluminum oxide (Al_2O_3) have been also used as pH-sensitive membranes because of their higher response [2, 3]. In general, the ISFET has several disadvantages such as low current sensitivity and device instability. On the contrary, the structure of the extended-gate field-effect transistor (EGFET) reveals many advantages over the conventional ISFET, such as the low cost, simple passivation and package, insensitivity of temperature and light, flexibility of shape of the extended-gate structure, and better long-term stability [4, 5]. EGFET explored by Van der Spiegel et al. in 1983 is a structure used to isolate FET from the chemical environment [6], in which a chemically sensitive membrane is deposited on the end of the signal line extended from the FET gate electrode. The surface ion adsorption mechanisms of pH-sensitive membranes in ISFET and EGFET are the same. The principal distinction between pH-ISFET and pH-EGFET sensors is the impedance of sensing films [7]. Insulating membranes, for example, SiO_2, Si_3N_4, and Al_2O_3, were commonly used for the fabrication of ISFET and presented very low sensitivities when applied in EGFET. The sensitively extended gate of EGFET must use a conductive material to be a sensing electrode that can transmit sensing signals easily [8–10]. Many materials were adopted as the pH-sensing membranes of pH-EGFET sensors, such as zinc oxide (ZnO) [11], tin oxide (SnO_2) [12], ruthenium oxide (RuO_2) [13], and vanadium oxide (V_2O_5)

[14]. Recently, one-dimensional ZnO nanostructures have attracted considerable attention as pH-sensitive membranes because of the unique advantages including high surface-to-volume ratio, nontoxicity, thermal stability, chemical stability, electrochemical activity, and high mechanical strength [15–17]. However, intrinsic ZnO exhibits larger sheet resistance and less conductivity. To achieve low impedance, it is necessary to increase the conductivity or reduce the resistivity of ZnO sensing membrane. ZnO nanostructures usually were doped with IIIA element, for instance, aluminum (Al) [18, 19], which could enhance their conductivities [20, 21]. Al-doped ZnO (AZO) nanowires (NWs) and nanotubes (NTs) have been presented for the high conductance and high crystal quality [22], which could be expected for lower resistivity. However, only the finite report demonstrates the pH-sensing properties of AZO nanostructures [23]. The stability and durability of AZO nanostructured pH-EGFET sensors have not been addressed. In this work, the pH-sensing and drift characteristics of hydrothermal Al-doped ZnO nanostructured pH-EGFET sensors were analytically demonstrated.

2. Experimental

The EGFET investigation is divided into two parts. One is the sensing unit containing the sensitive membrane, and the other is the MOSFET device. Figure 1 shows the key fabrication procedures of undoped ZnO and AZO nanostructures applied in pH-sensing membrane. The growth of undoped ZnO and AZO nanostructures on the glass substrate was performed by hydrothermal growth method. In the sensing unit, a 200 nm thick AZO film was sputtered on glass substrates to serve as a seed layer for the growth of undoped ZnO and AZO nanostructures. The precursor solution was prepared by mixing with 0.025 M zinc nitrate hexahydrate ($Zn(NO_3)_2{\cdot}6H_2O$) and 0.025 M hexamethylenetetramine (HMTA) in deionized water. The aluminum nitrate nonahydrate ($Al(NO_3)_3{\cdot}9H_2O$) powders were used as the doping source to add in the precursor solution. Then, the samples were placed in such a mixed hydrothermal solution at 85°C for 1 hour on a hot plate. The atomic ratio of Al dopant in the precursor solutions (Al/(Al+Zn)) was controlled as 0 at.% (undoped), 1 at.%, 2 at.%, 3 at.%, 5 at.%, and 7 at.%, respectively. After the hydrothermal method growth, the samples were bound to metal wire with silver paste and packaged with epoxy resin, and then the packaged electrode was put into an oven for 30 min at 120°C. Epoxy resin was used to avoid the leakage current and define the sensing window at $2 \times 2\,mm^2$. In addition, the Keithley 236 semiconductor parameter analyzer was used to measure the current-voltage (*I-V*) characteristics of the pH-EGFET sensor in pH 1, 3, 5, 7, 9, 11, and 13 phosphate buffer solutions. Figure 2(a) reveals the schema of pH-sensing measurement facility. A commercial Ag/AgCl electrode (DX200) was adopted as the standard reference electrode, offering a constant potential during the whole measuring process. The sensing unit and the reference electrode were directly immersed into the buffer solution and electrically connected to the gate of commercial standard MOSFET device (CD4007UB). To avoid the temperature effect due to outside light interference, measurements were carried out in a dark box at room temperature. Subsequently, response voltage and drift effect of the sensing device in different phosphate buffer solutions were measured with a specific voltage-time (*V-t*) measurement system (indicated in Figure 2(b)), which consists of a commercial instrument amplifier (LT1167) and a digital multimeter (HP 34401A). In this measurement system, the instrumentation amplifier was utilized to measure the total charges associated with the hydrogen ions accumulated on the sensing window, and its amplification gain is one. The output voltage variations versus time of the sensing unit were recorded with the reference electrode to provide constant voltage during the measurement process.

3. Results and Discussion

In the previous investigations [23, 24], the AZO nanostructures with various Al dosages were synthesized successfully on AZO/glass substrate by hydrothermal growth method at 85°C. The morphologies, crystallinity, optical emission properties, bonding states, and chemical compositions of AZO nanostructures show evident dependence on the Al dosage [24]. While the Al dosage was equal or less than 3 at.%, only NWs are observed. Both the undoped and lightly Al-doped ZnO NWs are well ordered and vertically aligned with similar specific dimensions (i.e., the average length of ~1 μm and diameter of ~ 100 nm). Contrarily, the nanosheets (NSs) are obtained while Al dosages are above 3 at.%. NWs and NSs coexisted when Al dosage was 5 at.%. The sample doped with 7 at.% Al dosage disclosures the remarkable changes on morphology, resulting in a complete NSs. The lightly Al-doped (≦3 at.%) NWs indicate single-crystalline wurtzite structure. On the contrary, the heavily Al-doped (i.e. 7 at.%) NSs reveal the polycrystalline ZnO wurtzite crystals. The optical emission properties of undoped ZnO and AZO nanostructures examined by photoluminescence (PL) spectra can be linked to the structural defects [24]. Less structural defects existed in the AZO NWs with appropriate Al dosage (i.e., 3 at.%). The reduced structural defects are probably related to the fact that the Al ions competed with Zn ions to consume the residual O ions and decrease the concentration of oxygen interstitials in the AZO NWs [25]. Furthermore, Al atoms may also have more opportunities to occupy the sites of oxygen vacancies in the AZO NWs, associated with the decreased concentration of oxygen vacancies [19]. The experimental compositions of Al in the AZO nanostructures were analyzed as 0 at.%, 0.31 at.%, 0.81 at.%, 1.98 at.%, 3.35 at.%, and 6.27 at.% by X-ray photoelectron spectroscopy (XPS, Physical Electronics PHI-1600) [23, 24], according to the controlled Al dosages of 0 at.%, 1 at.%, 2 at.%, 3 at.%, 5 at.%, and 7 at.% in the precursor solutions.

The operation of the pH-EGFET sensor is very similar to that of a conventional MOSFET, except that an additional sensing structure is immersed in the buffer solution. The relation between the pH value and drain-source current (I_{DS}) can be obtained by the basic MOSFET expression [26], where the threshold voltage of pH-EGFET sensor depends

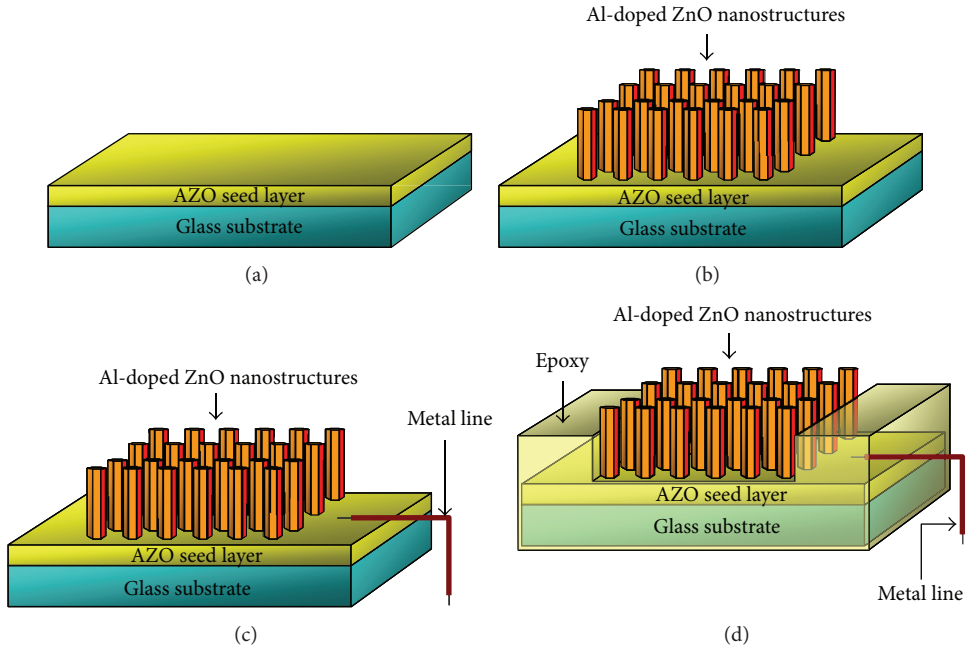

Figure 1: Key fabrication procedures of undoped ZnO and AZO nanostructures applied in pH-sensing membrane.

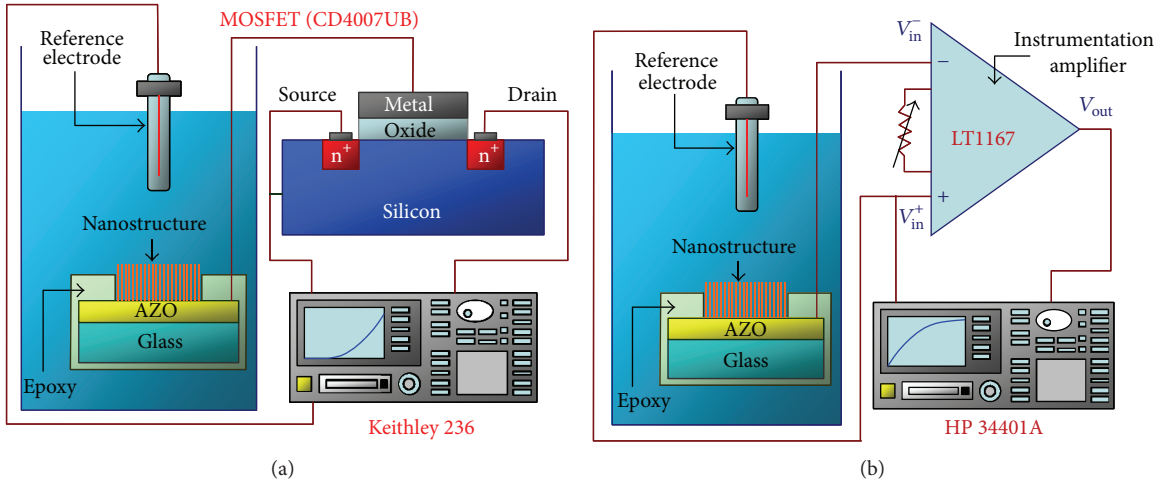

Figure 2: Schematic diagrams of the (a) *I-V* measurement facility and (b) *V-t* measurement system for the pH-EGFET sensors.

on the pH value. Figure 3 depicts the transfer characteristics (I_{DS}-V_{REF}) for the pH-EGFET sensors in the linear regime (when V_{DS} was fixed at 0.2 V) with pH values from 1 to 13. The I_{DS}-V_{REF} curves show that the threshold voltage shift ($\Delta V_{T(EGFET)}$) depends on the concentration of hydrogen ions. The threshold voltage moves from the left side to the right side of x-axis with a raised pH value similar to a decreased concentration of hydrogen ions. The flat-band voltage increases with the increasing of carrier concentration in sensing film [9], bringing about a diminution of pH-EGFET threshold voltage as the Al dosage rises, as shown in Figure 3. The pH sensitivity and linearity values can be extracted from the change in $V_{T(EGFET)}$ and can be written as follows:

$$\text{pH voltage sensitivity} = \left.\frac{V_{T(EGFET)}(x_2) - V_{T(EGFET)}(x_1)}{\text{pH}(x_2) - \text{pH}(x_1)}\right|_{I_{DS}=0.2\,\text{mA}} = \left.\frac{\Delta V_{T(EGFET)}}{\Delta \text{pH}}\right|_{I_{DS}=0.2\,\text{mA}}. \quad (1)$$

The pH sensitivity and linearity values were constructed from the relationship for V_{REF} as a function of pH (while

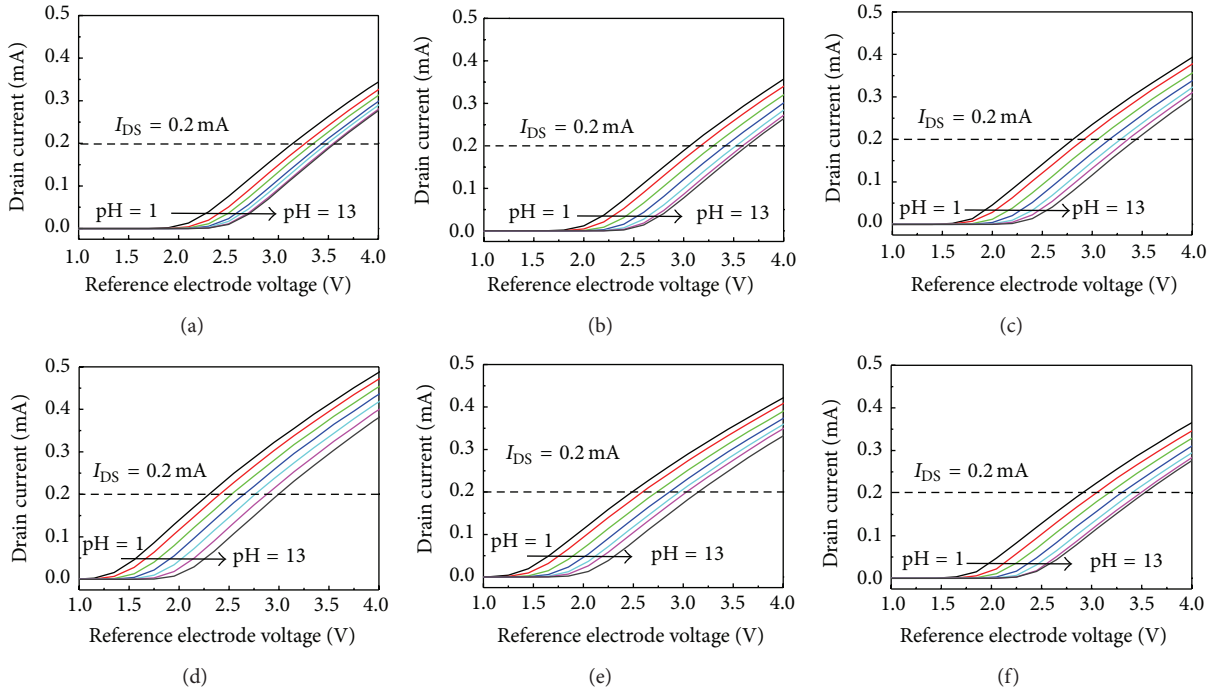

FIGURE 3: Transfer characteristics (I_{DS}-V_{REF}) for the pH-EGFET sensors in the linear regime with various Al dosages: (a) 0 at.%, (b) 1 at.%, (c) 2 at.%, (d) 3 at.%, (e) 5 at.%, and (f) 7 at.%.

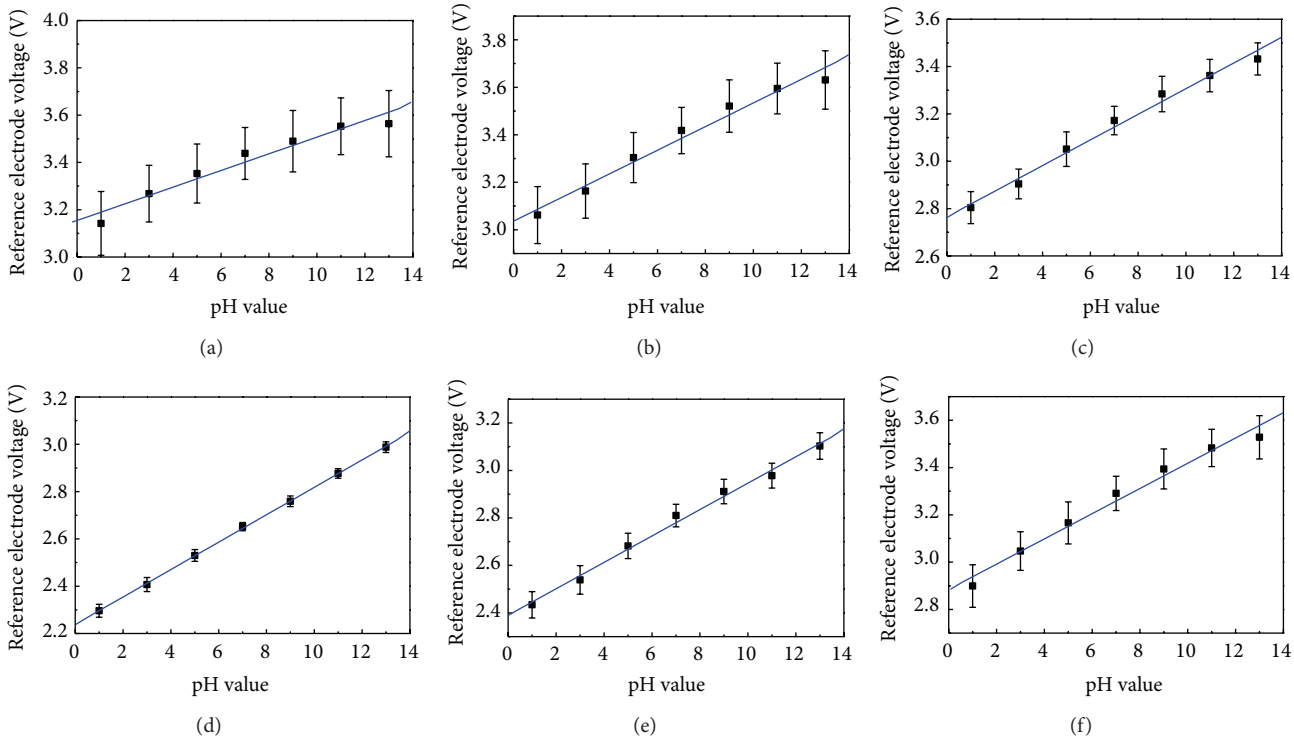

FIGURE 4: Linearity of the pH-EGFET sensors in the linear regime with various Al dosages while V_{DS} = 0.2 V and I_{DS} = 0.2 mA: (a) 0 at.%, (b) 1 at.%, (c) 2 at.%, (d) 3 at.%, (e) 5 at.%, and (f) 7 at.%.

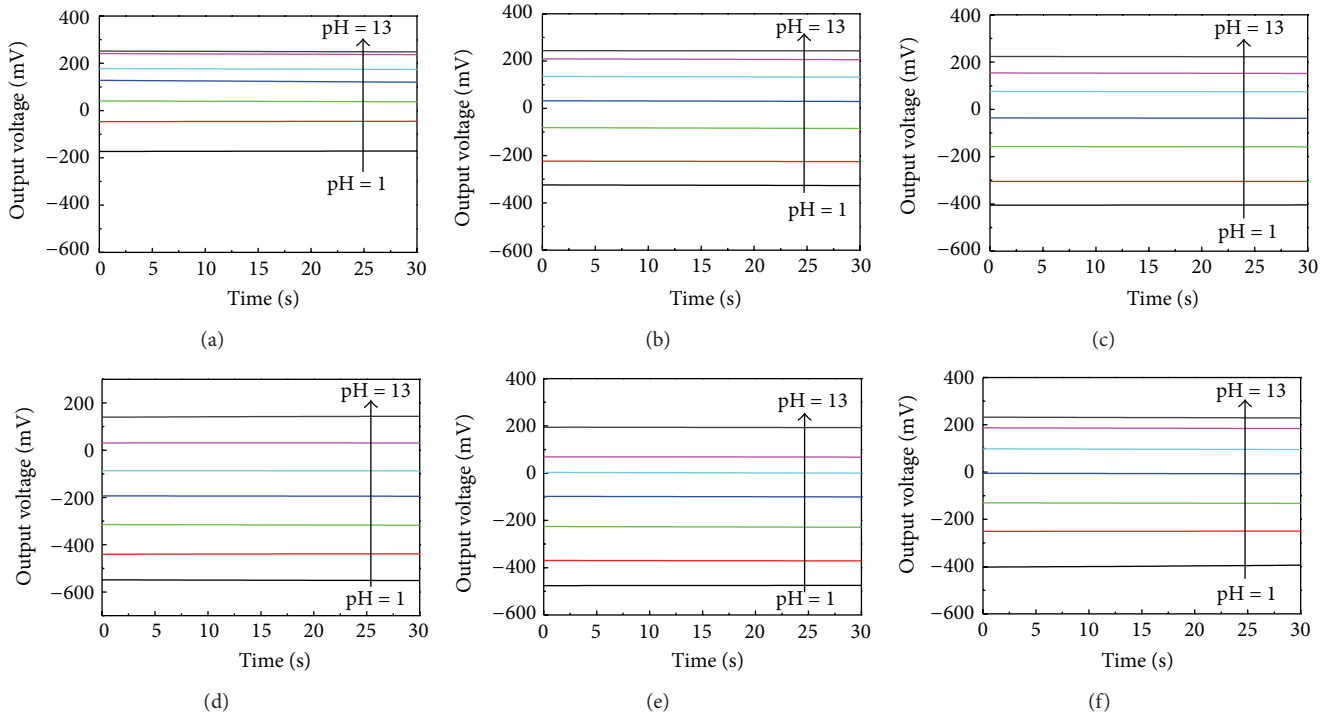

FIGURE 5: *V-t* curves of the pH-EGFET sensors immersed in pH 1~pH 13 buffer solutions with various Al dosages: (a) 0 at.%, (b) 1 at.%, (c) 2 at.%, (d) 3 at.%, (e) 5 at.%, and (f) 7 at.%.

I_{DS} was fixed at 0.2 mA), given in Figure 4. The pH voltage sensitivities are about 35.23, 49.79, 54.16, 57.95, 55.61, and 53.34 mV/pH with respect to the Al dosages of 0 at.%, 1 at.%, 2 at.%, 3 at.%, 5 at.%, and 7 at.% in the pH 1~pH 13 range, accordingly. Figure 4 exhibits the linearity of 0.9757, 0.9880, 0.9937, 0.9998, 0.9962, and 0.9902, correspondingly, for the Al dosages of 0 at.%~7 at.%. Furthermore, the deviation is about 0.126, 0.111, 0.068, 0.023, 0.054, and 0.084 V with respect to the Al dosages of 0~7 at.%, accordingly, based on the result of twenty measured samples. Moreover, the experimental sensitivity values can be consistent with the addressed observations of physical analysis [24]. The superior crystallinity and less structural defects can inhibit grain boundaries scattering and carrier trapping and result in the increases of carrier concentration and mobility, which can benefit for a better conductivity [27, 28]. Furthermore, the Fermi level is typically higher than the redox potential of the electrolyte for an n-type semiconductor electrode at open circuit [29]. After electrical contact, electrons will be transferred from the electrode into the solution. There is a positive charge associated with the space charge region and thus reflected in an upward bending of the band edges. The semiconductors have a significant density of structural defects between conduction band and valence band, presenting the pinning of Fermi level when contacting a liquid electrolyte solution [30].

Therefore, the structural defects play a role as similar as a junction of semiconductor metal. The density and energy distribution of structural defects determine their energy level or work function. The band bending degree of a semiconductor can be linked with the structural defects. Consequently, when the Al dosage was increased above 3 at.%, the sensitivity values are decreased significantly due to the polycrystalline and disorders of NSs. The readout circuit of the pH-EGFET sensor instrument amplifier is refered to in Figure 2(b). The change of the pH buffer solution will proportionally affect the interface potential of the solution and EGFET sensing membrane. The output signal can be expressed as

$$V_{OUT} = V_{IN}^{+} - V_{IN}^{-} = V_{REF} - V_{SENSING\text{-}FILM}, \quad (2)$$

where V_{IN}^{+} and V_{IN}^{-} are the two input terminal voltages of the instrumentation amplifier. V_{REF} and $V_{SENSING\text{-}FILM}$ are the voltages of reference electrode and the sensing film, which are connected to the input terminals of the instrumentation amplifier. Afterwards, the drift characteristics of the separate pH-EGFET sensors were obtained using this readout circuit. The drift effect has been used to evaluate durability and reliability of electrochemical sensors, especially for ISFETs, which relates to OH^{-} ions adsorption on sensing film surface in different buffer solutions [31].

Figures 5 and 6 demonstrate the *V-t* curves for short durations (i.e., 0~30 sec) and the drift characteristics of pH-EGFET sensors with long-term (i.e., 12 hours) measurement, respectively. The relation between output voltage and time is indicated in Figure 5 while the sensors were immersed in pH 1~pH 13 buffer solutions with various Al dosages. The response output voltage curves of the AZO pH-EGFET sensor with 3 at.% Al dosage are the most sensitive when compared to the others. The shifts in voltage from 5 to 12 hours were estimated to obtain the drift rate of pH-EGFET sensors immersed in buffer solutions. The long-term

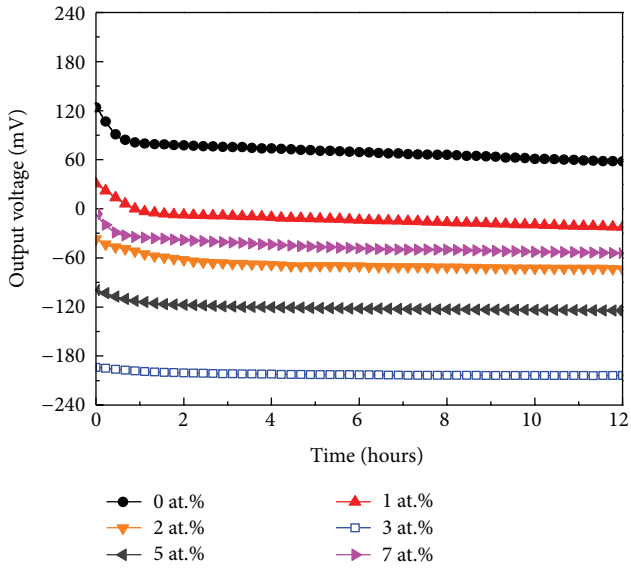

FIGURE 6: Drift characteristics of the undoped ZnO and AZO nanostructured pH-EGFET sensors measured within pH = 7 for the duration of 12 hours.

drift rates (revealed in Figure 6) of undoped ZnO and AZO nanostructures employed in pH-EGFET sensors are about 16.81, 13.59, 4.77, 1.27, 3.38, and 8.79 mV/hour with respect to the various Al dosages in pH 1~ pH 13 range, correspondingly. AZO nanostructures demonstrate smaller long-term drift rates (better durability and stability) than those of undoped ZnO nanostructures.

In brief, it suggests that AZO nanostructured pH-EGFET sensor with Al dosage of 3 at.% gives the best and most stable pH-sensing characteristics in this work. AZO nanostructured pH-EGFET sensor with 3 at.% Al dosage reveals the higher sensitivity of 57.95 mV/pH, the larger linearity of 0.9998, the smaller deviation of 0.023 in linearity, the lower drift rate of 1.27 mV/hour, the lower threshold voltage of 1.32 V, and the wider sensing range (i.e., pH 1~pH 13), which may be associated with the vertically well-aligned NWs array, superior crystallinity, less structural defects, and better conductivity [24]. The better conductivity of sensing electrode applied in EGFET can transmit sensing signals easily. Therefore, AZO nanostructured pH-EGFET sensors with 3 at.% Al dosage presents the optimum pH-sensing characteristics. The sensitively nanostructured membrane is also easy to fabricate and package. This result recommends that AZO nanostructured pH-EGFET sensors prepared by low-temperature hydrothermal growth method in the atmosphere demonstrate the promised sensing characteristics and can be candidates for the applications of disposable biosensors (i.e., glucose and urea sensor).

4. Conclusion

The AZO nanostructures with various Al dosages were synthesized on AZO/glass substrate by a simple hydrothermal growth method at a low temperature of 85°C. The pH-sensing properties of hydrothermal AZO nanostructures are evidently influenced by Al dosage. The AZO nanostructured pH-EGFET sensors with Al dosage of 3 at.% present the optimum pH-sensing characteristics in this work (i.e., the higher sensitivity of 57.95 mV/pH, the larger linearity of 0.9998, the smaller deviation of 0.023 in linearity, the lower drift rate of 1.27 mV/hour, the lower threshold voltage of 1.32 V, and the wider sensing range of pH 1~pH 13), which may be attributed to the vertically well-aligned NWs array, superior crystallinity, less structural defects, and better conductivity. Consequently, the well-aligned arrays of Al-doped ZnO NWs synthesised by hydrothermal growth method can disclose superior pH-sensing characteristics and be promising for the application of disposable biosensors.

Acknowledgments

This work was financially supported by the National Science Council of Taiwan under the Contract no. of NSC 101-2221-E-131-024. Thanks are also due to the Nano Facility Center (NFC) in National Chiao Tung University and the National Nano Device Laboratory (NDL) for the technical support.

References

[1] B. P. Bergveld, "Development of an ion sensitive solid-state device for neurophysiological measurement," *IEEE Transactions on Biomedical Engineering*, vol. 17, no. 1, pp. 70–71, 1970.

[2] M.-N. Niu, X.-F. Ding, and Q.-Y. Tong, "Effect of two types of surface sites on the characteristics of Si_3N_4-gate pH-ISFETs," *Sensors and Actuators B*, vol. 37, no. 1-2, pp. 13–17, 1996.

[3] L. Bousse, H. H. van den Vlekkert, and N. F. de Rooij, "Hysteresis in Al_2O_3-gate ISFETs," *Sensors and Actuators B*, vol. 2, no. 2, pp. 103–110, 1990.

[4] J.-C. Chou, J.-L. Chiang, and W. U. Chin-Lung, "PH and procaine sensing characteristics of extended-gate field-effect transistor based on indium tin oxide glass," *Japanese Journal of Applied Physics 1*, vol. 44, no. 7, pp. 4838–4842, 2005.

[5] N. H. Chou, J. C. Chou, T. P. Sun, and S. K. Hsiung, "Differential type solid-state urea biosensors based on ion-selective electrodes," *Sensors and Actuators B*, vol. 130, no. 1, pp. 359–366, 2008.

[6] J. van der spiegel, I. Lauks, P. Chan, and D. Babic, "The extended gate chemically sensitive field effect transistor as multi-species microprobe," *Sensors and Actuators*, vol. 4, pp. 291–298, 1983.

[7] J.-L. Chiang, J.-C. Chou, and Y.-C. Chen, "Study of the pH-ISFET and EnFET for biosensor applications," *Journal of Medical and Biological Engineering*, vol. 21, no. 3, pp. 135–146, 2001.

[8] L.-T. Yin, J.-C. Chou, W.-Y. Chung, T.-P. Sun, and S.-K. Hsiung, "Study of indium tin oxide thin film for separative extended gate ISFET," *Materials Chemistry and Physics*, vol. 70, no. 1, pp. 12–16, 2001.

[9] J.-C. Chou and C.-W. Chen, "Fabrication and application of ruthenium-doped titanium dioxide films as electrode material for ion-sensitive extended-gate FETs," *IEEE Sensors Journal*, vol. 9, no. 3, pp. 277–284, 2009.

[10] P. D. Batista and M. Mulato, "Polycrystalline fluorine-doped tin oxide as sensoring thin film in EGFET pH sensor," *Journal of Materials Science*, vol. 45, no. 20, pp. 5478–5481, 2010.

[11] P. D. Batista and M. Mulato, "ZnO extended-gate field-effect transistors as pH sensors," *Applied Physics Letters*, vol. 87, no. 14, Article ID 143508, 2005.

[12] P. D. Batista, M. Mulato, C. F. D. O. Graeff, F. J. R. Fernandez, and F. D. C. Marques, "SnO_2 extended gate field-effect transistor as pH sensor," *Brazilian Journal of Physics*, vol. 36, no. 2, pp. 478–481, 2006.

[13] J. C. Chou and D. J. Tzeng, "Study on the characteristics of the ruthenium oxide pH electrode," *Rare Metal Materials and Engineering*, vol. 35, p. 256, 2006.

[14] E. M. Guerra, G. R. Silva, and M. Mulato, "Extended gate field effect transistor using V_2O_5 xerogel sensing membrane by sol-gel method," *Solid State Sciences*, vol. 11, no. 2, pp. 456–460, 2009.

[15] Q. H. Li, Q. Wan, Y. J. Chen, T. H. Wang, H. B. Jia, and D. P. Yu, "Stable field emission from tetrapod-like ZnO nanostructures," *Applied Physics Letters*, vol. 85, no. 4, pp. 636–638, 2004.

[16] Q. Zhao, H. Z. Zhang, Y. W. Zhu et al., "Morphological effects on the field emission of ZnO nanorod arrays," *Applied Physics Letters*, vol. 86, no. 20, Article ID 203115, 2005.

[17] N. S. Ramgir, I. S. Mulla, K. Vijayamohanan et al., "Ultralow threshold field emission from a single multipod structure of ZnO," *Applied Physics Letters*, vol. 88, no. 4, Article ID 042107, 2006.

[18] D. F. Paraguay, M. Miki-Yoshida, J. Morales, J. Solis, and L. W. Estrada, "Influence of Al, In, Cu, Fe and Sn dopants on the response of thin film ZnO gas sensor to ethanol vapour," *Thin Solid Films*, vol. 373, no. 1-2, pp. 137–140, 2000.

[19] R.-C. Wang, C.-P. Liu, J.-L. Huang, and S.-J. Chen, "Single-crystalline AlZnO nanowires/nanotubes synthesized at low temperature," *Applied Physics Letters*, vol. 88, no. 2, Article ID 023111, 3 pages, 2006.

[20] S. Y. Bae, H. W. Seo, and J. Park, "Vertically aligned sulfur-doped ZnO nanowires synthesized via chemical vapor deposition," *Journal of Physical Chemistry B*, vol. 108, no. 17, pp. 5206–5210, 2004.

[21] J. Zhong, S. Muthukumar, Y. Chen et al., "Ga-doped ZnO single-crystal nanotips grown on fused silica by metalorganic chemical vapor deposition," *Applied Physics Letters*, vol. 83, no. 16, pp. 3401–3403, 2003.

[22] J. Chen, W. Lei, W. Chai, Z. Zhang, C. Li, and X. Zhang, "High field emission enhancement of ZnO-nanorods via hydrothermal synthesis," *Solid-State Electronics*, vol. 52, no. 2, pp. 294–298, 2008.

[23] P.-Y. Yang, J.-L. Wang, P.-C. Chiu et al., "PH sensing characteristics of extended-gate field-effect transistor based on al-doped ZnO nanostructures hydrothermally synthesized at low temperatures," *IEEE Electron Device Letters*, vol. 32, no. 11, pp. 1603–1605, 2011.

[24] P.-Y. Yang, J.-L. Wang, W.-C. Tsai et al., "Field-emission characteristics of Al-doped ZnO nanostructures hydrothermally synthesized at low temperature," *Journal of Nanoscience and Nanotechnology*, vol. 11, no. 7, pp. 6013–6019, 2011.

[25] H. W. Kim, M. A. Kebede, and H. S. Kim, "Structural, Raman, and photoluminescence characteristics of ZnO nanowires coated with Al-doped ZnO shell layers," *Current Applied Physics*, vol. 10, no. 1, pp. 60–63, 2010.

[26] S. M. Sze, *Physics of Semiconductor Devices*, John Wiley & Sons, New York, NY, USA, 2nd edition, 1981.

[27] X. T. Hao, J. Ma, D. H. Zhang et al., "Thickness dependence of structural, optical and electrical properties of ZnO:Al films prepared on flexible substrates," *Applied Surface Science*, vol. 183, no. 1-2, pp. 137–142, 2001.

[28] H. Kim, J. S. Horwitz, G. Kushto et al., "Effect of film thickness on the properties of indium tin oxide thin films," *Journal of Applied Physics*, vol. 88, no. 10, pp. 6021–6025, 2000.

[29] S. Al-Hilli and M. Willander, "The pH response and sensing mechanism of n-type ZnO/electrolyte interfaces," *Sensors*, vol. 9, no. 9, pp. 7445–7480, 2009.

[30] R. L. Van Meirhaeghe, F. Cardon, and W. P. Gomes, "A quantitative expression for partial Fermi level pinning at semiconductor/redox electrolyte interfaces," *Journal of Electroanalytical Chemistry*, vol. 188, no. 1-2, pp. 287–291, 1985.

[31] S. Jamasb, S. Collins, and R. L. Smith, "A physical model for drift in pH ISFETs," *Sensors and Actuators B*, vol. B49, no. 1-2, pp. 146–155, 1998.